Inhibition of thrombocyte activation restores protective immunity to mycobacterial infection

Elinor Hortle[1], Khelsey E. Johnson[2], Matt D. Johansen[1], Tuong Nguyen[1], Jordan A. Shavit[3], Warwick J. Britton[1,4], David M. Tobin[2], Stefan H. Oehlers[1,4] *

[1] Tuberculosis Research Program, Centenary Institute, University of Sydney, Camperdown, NSW 2050, Australia

[2] Department of Molecular Genetics and Microbiology, Duke University School of Medicine, Durham, NC 27710, USA

[3] Department of Pediatrics and Cellular and Molecular Biology Program, University of Michigan, Ann Arbor, MI 48107, USA

[4] Central Clinical School and Marie Bashir Institute, The University of Sydney, Camperdown, NSW 2050, Australia

* Corresponding author email: s.oehlers@centenary.org.au, Twitter: @oehlerslab

Summary

Infection-induced thrombocytosis is a clinically important complication of tuberculosis infection. Recent studies have highlighted the utility of aspirin as a host-directed therapy modulating the inflammatory response to infection, but have not investigated the possibility that the effect of aspirin is related to an anti-platelet mode of action. Here we utilise the zebrafish-*Mycobacterium marinum* model to show mycobacteria drive host haemostasis through the formation of granulomas. Treatment of infected zebrafish with aspirin markedly reduced mycobacterial burden. This effect is reproduced by treatment with platelet-specific glycoprotein IIb/IIIa inhibitors demonstrating a detrimental role for infection-induced thrombocyte activation. We find that the reduction in mycobacterial burden is dependent on

macrophages and granuloma formation providing the first *in vivo* experimental evidence that infection-induced platelet activation compromises protective host immunity to mycobacterial infection. Our study illuminates platelet activation as an efficacious target of aspirin, a widely available and affordable host-directed therapy candidate for tuberculosis.

Keywords

Mycobacterial infection, haemostasis, innate immunity, clotting

Introduction

Mycobacterium tuberculosis is the world's most lethal pathogen, causing nearly 2 million deaths each year (World Health Organization. and Global Tuberculosis Programme.). The increasing incidence of both multi- and extremely-drug resistant tuberculosis (TB) urgently require the development of therapeutics that overcome the shortcomings of conventional antibiotics. Pathogenic mycobacteria co-opt numerous host pathways to establish persistent infection, and subversion of these interactions with host-directed therapies (HDTs) has been shown to reduce the severity of infection in animal models. For example, we have recently shown that mycobacteria induce host angiogenesis and increase host vascular permeability; blockade of either of these processes reduced both the growth and spread of bacteria (Oehlers et al., 2017; Oehlers et al., 2015). Therefore, host processes co-opted by the bacteria provide attractive targets for novel TB treatments. One such pathway may be haemostasis.

Thrombocytosis has long been recognised as a biomarker for advanced TB, and infection is often accompanied by the induction of a hyper-coagulable state, resulting in increased risk of deep vein thrombosis and stroke (Kutiyal et al., 2017; Robson et al., 1996). Recent evidence hints that mycobacteria may drive this process, and that it may aid their growth. For example,

cell wall components from *M. tuberculosis* can induce expression of tissue factor - an important activator of coagulation - in macrophages (Kothari et al., 2012). In mice and humans markers of platelet activation are upregulated during *M. tuberculosis* infection (Fox et al., 2018), and it has been shown *in vitro* that interaction with activated platelets increases the conversion of infected macrophages into cells permissive for bacterial growth (Feng et al., 2014; Fox et al., 2018). To date the pathogenic roles of haemostasis have not been studied in an intact *in vivo* model of mycobacterial infection.

Here we used the zebrafish-*M. marinum* model to investigate the role of host thrombocytes in mycobacterial infection. We show evidence that coagulation and thrombocyte activation are both driven by mycobacteria, and that infection-induced activation of thrombocytes compromises protective immunity. However, clot formation itself has no effect on infection suggesting direct communication between the mycobacterial infection milieu and thrombocytes.

Results

Mycobacterium marinum induces coagulation in zebrafish.

To determine if *M. marinum* induces coagulation in zebrafish, we infected *Tg(fabp10a:fgb-EGFP)* transgenic embryos expressing EGFP-tagged fibrinogen beta (FGB) with *M. marinum*-tdtomato, and imaged the developing infection every 15 minutes from 3 days post infection (DPI), until 6 DPI (Supplementary Video 1). We observed that clots formed only at areas of bacterial growth, and that the size of the clots increased as the number of bacteria

increased over the course of the infection (Figure 1A). When we infected fish with ΔESX1 mutant *M. marinum*, which lacks the ability to export key virulence proteins and does not form granulomas, significantly reduced clot formation was observed (Figures 1B-C). Together, these data demonstrate that coagulation is a conserved consequence of infection driven by pathogenic mycobacteria across host species. Treatment with the anti-coagulant warfarin to prevent clot formation during infection did not affect bacterial burden, suggesting coagulation does not affect bacterial growth within the host (Figures 1D-E and S1).

Mycobacterium marinum induces thrombosis in zebrafish.

To determine if *M. marinum* induces thrombosis in zebrafish, we infected *Tg(cd41:GFP)* embryos, where thrombocytes are marked by GFP expression, with red fluorescent *M. marinum*. Infected embryos had significantly increased density of thrombocytes around the tail venous plexus where granulomas preferentially form (Figures 1F and S1A-B). Amongst infected embryos, there was a strong positive correlation between thrombocyte density and mycobacterial burden (Figure S1C). This increased thrombocyte density, and the positive correlation between density and burden, were also observed in ΔESX1 mutant *M. marinum* infection (Figures S1D-E), indicating that mycobacteria-induced thrombosis is ESX1 independent.

Because the *cd41* promoter is active in non-motile thrombocyte precursors within their caudal haematopoietic tissue, we could not conclusively determine if these thrombocytes had actively migrated to and been retained at the site of infection (Lin et al., 2005). To determine if zebrafish thrombocytes are recruited to sites of mycobacterial infection, we performed trunk injection of *M. marinum* in *Tg(cd41:GFP)* at 3 days post fertilization (DPF), a time point after which mature thrombocytes are in the circulation. Embryos were then imaged at 2,

3, and 4 DPI. Thrombocytes were co-localised with the sites of infection in 87% of fish. Rather than forming a stable and growing clot over a period of days (as we observed for FGB), thrombocytes appeared to form transient associations with sites of infection (Figure S3). In some instances, new thrombocytes seemed to be retained at sites of infection in different locations each day, and in others, thrombocytes appeared to stay stationary for multiple days (Figure S3). The size of infection-associated thrombocytes varied greatly, suggesting activation and progressive degranulation or death of thrombocytes at sites of infection. Thrombocytes were most often observed on the edges of granulomas consistent with the location of granuloma-defining macrophages (Cronan et al., 2016). Therefore thrombocyte-granuloma interactions appear to be a conserved feature of mycobacterial infection across species.

Anti-platelet drugs reduce mycobacterial burden in zebrafish.

To determine if the previously reported infection-controlling effect of aspirin is conserved across vertebrate species (Mai et al., 2018), we treated *M. marinum*-infected fish with aspirin by immersion. Mycobacterial burden was reduced by approximately 50% in aspirin-treated embryos (Figure 2A).

Although aspirin is a widely used platelet inhibitor, it is a broadly acting nonsteroidal anti-inflammatory drug that is known to modulate infection-relevant prostaglandin metabolism. Thus, to determine if the anti-platelet effects of aspirin treatment contribute to the reduced mycobacterial burden, we treated *M. marinum*-infected fish with the platelet-specific, small molecule Glycoprotein IIb/IIIa inhibitors, tirofiban or eptifibatide. Treatment with either Glycoprotein IIb/IIIa inhibitor phenocopied aspirin by reducing bacterial burden providing

the first direct evidence of a detrimental role for platelet activation in the immune response to mycobacterial infection (Figure 2B-C).

Surprisingly, tirofiban treatment resulted in significantly higher number of visible thrombocytes at sites of infection compared to controls (Figures 2D-E). This suggests that, in contrast to our observations in the tail wound thrombosis model, tirofiban does not inhibit thrombocyte migration to areas of bacterial infection, but may act by preventing activation and subsequent degranulation or death of zebrafish thrombocytes in response to mycobacterial infection.

We next examined the cellular target of anti-platelet drugs in our infection system. We performed antibacterial testing of the anti-platelet drugs in axenic cultures of *M. marinum* and did not observe any effect on bacterial growth *in vitro* demonstrating host-directed activity (Figure 2F).

The specificity of anti-platelet drugs against mycobacterial infection was tested in acute *Pseudomonas aeruginosa* infection. Treatment of *P. aeruginosa*-infected embryos with either class of anti-platelet drug did not affect survival demonstrating specificity against chronic mycobacterial infection (Figure 2G).

The anti-bacterial effect of anti-platelet drugs is thrombocyte dependent.

We next confirmed that anti-platelet drugs inhibit thrombocyte activation in zebrafish using a tail wound thrombosis assay (Figure S4A). Anti-platelet drugs reduced the number of thrombocytes recruited to tail wound clots demonstrating conservation of cellular target in zebrafish embryos (Figure S4B-C). Of the two Glycoprotein IIb/IIIa inhibitors tirofiban and

eptifibatide, tirofiban is the more stable small molecule. Therefore we chose to use tirofiban for inhibition of thrombocytes in all further experiments.

To determine if zebrafish thrombocytes are the conserved target for tirofiban in the zebrafish-*M. marinum* infection model, we inhibited thrombopoiesis by injection with a morpholino against the thrombopoietin receptor *cmpl* (Lin et al., 2005). Surprisingly, inhibition of thrombopoiesis did not affect the outcome of infection. However, tirofiban treatment failed to reduce bacterial burden in thrombocyte-depleted embryos, demonstrating thrombocytes are the cellular target of this drug in the zebrafish infection model (Figure 3A).

To confirm that tirofiban was acting specifically through inhibition of Glycoprotein IIb/IIIa, we performed infection experiments in Glycoprotein IIb/IIIa knock-out (KO) transgenic embryos (*itga2b* mutants). The *itga2b*^{sa10134} allele caused a dose-dependent reduction in thrombocytes recruited to tail wound clots (Figure S4A). As with *cmpl* knockdown, complete KO of *itga2b* had no effect on bacterial burden (Figure 3F), and thrombocyte accumulation at the site of infection was also unaffected (Figures S4B-C). However, heterozygous embryos phenocopied tirofiban treatment, showing a trend to reduced bacterial burden and increased thrombocyte accumulation (Figures 3B and S4B-C). This suggests that treatment with tirofiban may only partially inhibit Glycoprotein IIb/IIIa in our model.

Thrombocyte activation and coagulation are independently induced by mycobacterial infection.

We hypothesised that infection-induced coagulation and the resulting fibrin deposition in clots would activate thrombocytes through fibrin cross-linking. To investigate this hypothesis, we

again used warfarin, which prevented clot formation during infection and did not affect bacterial burden (Figure 1E). However, the addition of warfarin to our tirofiban treatment model had no effect on the ability of tirofiban to reduce bacterial burden (Figure 3C).

To discount the possibility that warfarin and tirofiban co-treatment resulted in non-specific toxicity, we utilised a *fibrinogen alpha chain* mutant zebrafish line that does not readily form clots. Tirofiban treatment of FGA mutant zebrafish still significantly reduced bacterial burden further demonstrating that infection-induced activation of coagulation is not upstream of thrombocyte activation by mycobacterial infection (Figure 3D).

Conversely, we next asked if thrombocyte activation contributes to infection-induced coagulation. Analysis of FGB-GFP clots in tirofiban-treated embryos revealed reduced total clot formation (Figure 3E). However, correction for relative bacterial burden revealed that the reduced clot formation was a burden-dependent and thrombus formation was not additionally impacted by tirofiban treatment (Figure 3F).

Thrombocyte activation compromises immunity through granuloma-associated macrophages.

To further delineate the mechanism by which thrombocyte activation compromises innate immune control of mycobacterial infection but not the response to *Pseudomonas* infection, we asked if granuloma formation and maturation is essential to pathological thrombocyte activation.

To examine the requirement of granuloma formation and necrosis for thrombocyte-inhibiting drug efficacy, we infected embryos with ΔESX1 *M. marinum* that are unable to drive granuloma

maturation or necrosis. Tirofiban treatment had no effect on mutant bacterial burden at 5 DPI (Figure 4A). Similarly, in embryos infected with *M. marinum* at a dose too low to form necrotic granulomas by 5 DPI, continuous tirofiban treatment had no effect on bacterial burden at 5 DPI (Figure S6A).

We next took advantage of the stereotypical progression of innate immune granulomas in zebrafish embryos to investigate the temporal activity of thrombocyte inhibition by tirofiban. We found that at 3 DPI, a time-point with nascent granuloma formation but prior to significant granuloma organisation and necrosis, tirofiban had no effect on bacterial burden (Figure 4B). Conversely, treatment of infection from 4 to 5 DPI, a time-point when granulomas are organised and start to become necrotic, tirofiban significantly reduced bacterial burden within 24 hours (Figure 4C).

Macrophages are key cells in the innate granuloma, therefore to determine if thrombocyte inhibition exerts a protective effect through boosting macrophage-dependent immunity, we to depleted macrophages. We injected clodronate liposomes to deplete macrophages early during granuloma formation at 3 DPI (Figure S6B-C). Anti-platelet drug treatment was started immediately after liposome injection. In macrophage-depleted fish tirofiban did not reduce bacterial burden (Figure 4D).

It has previously been shown that in the presence of mycobacteria *in vitro*, platelets accelerate the conversion of macrophages to foam cells, which are permissive for mycobacterial growth, suggesting a mechanism for infection-induced thrombocytosis to compromise innate immunity to mycobacterial infection (Feng et al., 2014). We therefore hypothesised that thrombocyte inhibition would reduce the conversion of macrophages into

foam cells. We investigated this by performing Oil-red O staining to measure lipid accumulation within individual granulomas (Figure 4E). Because tirofiban treatment reduced bacterial burden, Oil-red O density was only compared between size-matched granulomas in treatment group. Tirofiban-treated embryos had significantly less Oil-red O accumulation in their granulomas when compared to DMSO control, even after correction for reduced bacterial burden (Figure 4F). Together, these data demonstrate an *in vivo* effect of thrombocyte activation inhibiting an effective immune response by converting macrophages into foam cells in mycobacterial granuloma.

Given that foam cell formation is closely associated with necrosis in tuberculosis (Russell et al., 2009) we hypothesised that tirofiban treatment would reduce cell death within the granuloma. We therefore used TUNEL staining to detect the fragmented DNA of dying cells in *M. marinum* infected embryos. At 5 DPI, tirofiban-treated embryos showed significantly less TUNEL staining, indicating significantly reduced cell death within the granuloma (Figures 4G-H). Together these results indicate that infection-induced platelet activation aggravates a basal rate of macrophage cell death in the granuloma.

Discussion

Here we have used the zebrafish-*M. marinum* model to identify infection-induced haemostasis as a detrimental host response that is co-opted by pathogenic mycobacteria. Our data builds on previous studies that have shown coagulation, thrombocytosis and thrombocyte activation are associated with mycobacterial infection, and provide the first *in vivo* study to demonstrate a direct role for thrombocyte activation in promoting mycobacterial growth. We have shown that infection-induced haemostasis is conserved in the zebrafish-*M.*

252 *marinum* infection model, and that the platelet inhibiting drugs, aspirin, tirofiban, and
253 eptifibatide, are able to reduce bacterial burden, independently of effects on coagulation,
254 through host-mediated effects (Graphical abstract).
255
256 A number of studies have investigated aspirin as a possible adjunctive treatment for TB in
257 both mice and humans (reviewed in (Hawn et al., 2013; Kalantri and Kalantri, 2018; Kroesen
258 et al., 2017; Kroesen et al., 2018)). The results of these studies have been far from
259 conclusive, with some finding beneficial effects, others finding no effect, and still others
260 finding aspirin may reduce the effectiveness of anti-tubercular drugs. This lack of consensus
261 may be due to the fact that NSAIDs affect many cell types and processes important for the
262 host response to mycobacterial infection, not just coagulation and platelet activation. Our
263 study expands this literature by demonstrating a significant reduction in mycobacterial burden
264 following treatment with two specific anti-platelet drugs, tirofiban and eptifibatide, in addition to
265 aspirin.
266
267 Our study found that coagulation and thrombocytes are independently activated by infection
268 and have distinct roles during the pathogenesis of mycobacterial infection of zebrafish.
269 Inhibiting coagulation alone did not significantly reduce bacterial burden, and therefore we
270 considered anti-platelet treatment as a more attractive HDT than anti-coagulant treatment.
271 Although we found lower total clot formation in tirofiban-treated embryos, this was only
272 proportional to bacterial load, suggesting infection-induced coagulation could be independent of
273 infection-induced thrombocyte activation. It must be noted that we only measure a simple single
274 end-point in our zebrafish embryo experiments (bacterial load) at a relatively early time point for
275 a chronic infection. In more complex animals, where stroke and DVT are important secondary
276 complications of mycobacterial infection, reducing coagulation may yet prove to be efficacious

277 as a HDT during TB therapy to reduce morbidity. Conversely, data from the mouse model of TB
278 suggests tissue factor-induced fibrin is necessary to contain mycobacteria within granulomas
279 (Venkatasubramanian et al., 2016).
280
281 Our study provides evidence that infection-induced haemostasis is a conserved function of
282 the core mycobacterial pathogenicity program centred around granuloma formation. Our
283 experiments with ΔESX1 mutant *M. marinum*, which cannot secrete key virulence proteins
284 that drive granuloma formation, demonstrated ESX1-dependent haemostasis and
285 responsiveness to growth restriction by platelet inhibiting drugs. These data fit well with our
286 observations that stationary thrombocytes were only observed around well-developed
287 mycobacterial granulomas, and platelet inhibition was only effective at reducing bacterial
288 burden after the development of significant granuloma pathology. Together these results point
289 to a bidirectional relationship between thrombocyte activation and granuloma maturation
290 (Figure 6).
291
292 Interestingly we observed that tirofiban treatment increased the number of thrombocytes
293 accumulated at sites of infection. This may represent increased migration, increased
294 accumulation through coagulation or decreased activation and subsequent
295 degranulation/death. Given tirofiban blocks the glycoprotein IIb/IIIa integrin - on which
296 platelet migration is dependent (Gaertner et al., 2017) - and we observed that tirofiban
297 reduced migration of thrombocytes in our tail wound model, we do not consider that
298 increased migration is likely to be responsible. Similarly, an increase in coagulation
299 'trapping' thrombocytes at the site of infection is not supported by our experiments in
300 *Tg(fabp10a:fgb-EGFP)* transgenic embryos. We therefore propose that this 'increase'
301 actually represents a decrease in thrombocyte activation. Previous research has shown that

infection-activated platelets can undergo phagocytosis and/or apoptosis (Feng et al., 2014; Gaertner et al., 2017; Hottz et al., 2014); both of these processes would result in the loss of visible GFP+ thrombocytes from our system.

Recent research has highlighted the important role of platelets as innate immune cells; they are able to release anti-microbial peptides, pick up and 'bundle' bacteria, and initiate the recruitment of other innate immune cells to sites of infection (Gaertner et al., 2017; Li et al., 2017; Morrell et al., 2014). The low frequency at which direct thrombocyte-mycobacterial interactions were observed in our study argues against thrombocytes having a significant role in directly mediating immunity to mycobacterial infection. Our experiments demonstrating macrophage-dependence for anti-platelet drug mediated control of infection and reduced lipid accumulation in the granuloma suggest that infection-induced thrombocyte activation modulates macrophage containment of infection.

Our study joins several *in vitro* studies that have shown platelets can induce macrophages to have differential responses to bacteria or other pathologic stimuli. In the presence of *S. aureus*, thrombin-activated platelets induce macrophages to increase phagocytosis and slow the growth of bacteria (Ali et al., 2017). Conversely, platelets can supress the macrophage response to LPS (Ando et al., 2016), and induce macrophages to produce less TNF, more IL-10, and more IL-1ß in response to both BCG and *M. tuberculosis* (Feng et al., 2014; Fox et al., 2018). Crucially it has been shown that platelets are necessary for the formation of foam cells in the context of mycobacterial infection and atheroma (Feng et al., 2014). Our experiments with both Oil Red O and TUNEL staining demonstrate that thrombocytes induce similar pathways *in vivo* in response to *M. marinum*; directing macrophages towards foam-cell formation and necrosis.

Here we used the zebrafish-*M.marinum* model to show that mycobacteria drive coagulation and thrombosis through the formation of granulomas. We found that inhibition of thrombocyte activation was able to reduce foam-cell formation and cell death within the granuloma, leading to dramatically reduced bacterial burden. This is the first *in vivo* experimental evidence that infection-induced platelet activation contributes to the pathogenesis of mycobacterial infection. Our study identifies platelet activation as a potential target for tuberculosis host-directed therapy.

Acknowledgements

We thank Dr Kristina Jahn and Sydney Cytometry for assistance with imaging equipment; Garvan Biological Testing Facility staff Ms Jennifer Brand, Mr Michael Pickering, Ms Rola Bazzi, Dr Lucie Nedved and Dr Stephanie Allison at the Garvan Institute of Medical Research for maintenance of zebrafish breeding stock; and Professors Lalita Ramakrishnan, Shaun Jackson and Georges Grau, Associate Professor Carl Feng and Dr Jorn Coers for helpful discussion of results.

This work was supported by the Australian National Health and Medical Research Council APP1099912 and APP1053407; University of Sydney Fellowship; NSW Ministry of Health under the NSW Health Early-Mid Career Fellowships Scheme; and the Kenyon Family Inflammation Award (S.H.O.), Duke Summer Research Opportunities Program (K.J.), NIH Director's New Innovator Award 1DP2-OD008614 (D.M.T), NIH R01-HL124232 and R01-HL125774 (J.A.S.).

Author contributions

E.H., D.M.T. and S.H.O designed the experiments. E.H., K.E.J., M.D.J., T.N. and S.H.O performed the experiments. J.A.S. generated transgenic and mutant zebrafish lines. E.H. and S.O. wrote the paper. W.J.B., D.M.T. and S.H.O. supervised the project.

Declaration of Interests

The authors declare no competing interests.

References

Ali, R.A., Wuescher, L.M., Dona, K.R., and Worth, R.G. (2017). Platelets Mediate Host Defense against Staphylococcus aureus through Direct Bactericidal Activity and by Enhancing Macrophage Activities. J Immunol *198*, 344-351.

Ando, Y., Oku, T., and Tsuji, T. (2016). Platelets attenuate production of cytokines and nitric oxide by macrophages in response to bacterial endotoxin. Platelets *27*, 344-350.

Cronan, M.R., Beerman, R.W., Rosenberg, A.F., Saelens, J.W., Johnson, M.G., Oehlers, S.H., Sisk, D.M., Jurcic Smith, K.L., Medvitz, N.A., Miller, S.E., *et al.* (2016). Macrophage Epithelial Reprogramming Underlies Mycobacterial Granuloma Formation and Promotes Infection. Immunity *45*, 861-876.

Feng, Y., Dorhoi, A., Mollenkopf, H.J., Yin, H., Dong, Z., Mao, L., Zhou, J., Bi, A., Weber, S., Maertzdorf, J., *et al.* (2014). Platelets direct monocyte differentiation into epithelioid-like multinucleated giant foam cells with suppressive capacity upon mycobacterial stimulation. J Infect Dis *210*, 1700-1710.

375 Fox, K.A., Kirwan, D.E., Whittington, A.M., Krishnan, N., Robertson, B.D., Gilman, R.H.,
376 Lopez, J.W., Singh, S., Porter, J.C., and Friedland, J.S. (2018). Platelets Regulate Pulmonary
377 Inflammation and Tissue Destruction in Tuberculosis. Am J Respir Crit Care Med.
378 Gaertner, F., Ahmad, Z., Rosenberger, G., Fan, S., Nicolai, L., Busch, B., Yavuz, G.,
379 Luckner, M., Ishikawa-Ankerhold, H., Hennel, R., *et al.* (2017). Migrating Platelets Are
380 Mechano-scavengers that Collect and Bundle Bacteria. Cell *171*, 1368-1382 e1323.
381 Hawn, T.R., Matheson, A.I., Maley, S.N., and Vandal, O. (2013). Host-directed therapeutics
382 for tuberculosis: can we harness the host? Microbiol Mol Biol Rev *77*, 608-627.
383 Hottz, E.D., Medeiros-de-Moraes, I.M., Vieira-de-Abreu, A., de Assis, E.F., Vals-de-Souza,
384 R., Castro-Faria-Neto, H.C., Weyrich, A.S., Zimmerman, G.A., Bozza, F.A., and Bozza, P.T.
385 (2014). Platelet activation and apoptosis modulate monocyte inflammatory responses in
386 dengue. J Immunol *193*, 1864-1872.
387 Johansen, M.D., Kasparian, J.A., Hortle, E., Britton, W.J., Purdie, A.C., and Oehlers, S.H.
388 (2018). Mycobacterium marinum infection drives foam cell differentiation in zebrafish
389 infection models. bioRxiv.
390 Kalantri, A., and Kalantri, S. (2018). Can aspirin help? Elife *7*.
391 Kothari, H., Rao, L.V., Vankayalapati, R., and Pendurthi, U.R. (2012). Mycobacterium
392 tuberculosis infection and tissue factor expression in macrophages. PLoS ONE *7*, e45700.
393 Kroesen, V.M., Groschel, M.I., Martinson, N., Zumla, A., Maeurer, M., van der Werf, T.S.,
394 and Vilaplana, C. (2017). Non-Steroidal Anti-inflammatory Drugs As Host-Directed Therapy
395 for Tuberculosis: A Systematic Review. Front Immunol *8*, 772.
396 Kroesen, V.M., Rodriguez-Martinez, P., Garcia, E., Rosales, Y., Diaz, J., Martin-Cespedes,
397 M., Tapia, G., Sarrias, M.R., Cardona, P.J., and Vilaplana, C. (2018). A Beneficial Effect of
398 Low-Dose Aspirin in a Murine Model of Active Tuberculosis. Front Immunol *9*, 798.

399 Kutiyal, A.S., Gupta, N., Garg, S., and Hira, H.S. (2017). A Study of Haematological and
400 Haemostasis Parameters and Hypercoagulable State in Tuberculosis Patients in Northern
401 India and the Outcome with Anti-Tubercular Therapy. Journal of clinical and diagnostic
402 research : JCDR *11*, OC09-OC13.
403 Li, J.L., Zarbock, A., and Hidalgo, A. (2017). Platelets as autonomous drones for hemostatic
404 and immune surveillance. J Exp Med.
405 Lin, H.F., Traver, D., Zhu, H., Dooley, K., Paw, B.H., Zon, L.I., and Handin, R.I. (2005).
406 Analysis of thrombocyte development in CD41-GFP transgenic zebrafish. Blood *106*, 3803-
407 3810.
408 Mai, N.T., Dobbs, N., Phu, N.H., Colas, R.A., Thao, L.T., Thuong, N.T., Nghia, H.D., Hanh,
409 N.H., Hang, N.T., Heemskerk, A.D., *et al.* (2018). A randomised double blind placebo
410 controlled phase 2 trial of adjunctive aspirin for tuberculous meningitis in HIV-uninfected
411 adults. eLife *7*.
412 Matty, M.A., Oehlers, S.H., and Tobin, D.M. (2016). Live Imaging of Host-Pathogen
413 Interactions in Zebrafish Larvae. Methods Mol Biol *1451*, 207-223.
414 Morrell, C.N., Aggrey, A.A., Chapman, L.M., and Modjeski, K.L. (2014). Emerging roles for
415 platelets as immune and inflammatory cells. Blood *123*, 2759-2767.
416 Oehlers, S.H., Cronan, M.R., Beerman, R.W., Johnson, M.G., Huang, J., Kontos, C.D., Stout,
417 J.E., and Tobin, D.M. (2017). Infection-induced vascular permeability aids mycobacterial
418 growth. J Infect Dis *215*, 813-817.
419 Oehlers, S.H., Cronan, M.R., Scott, N.R., Thomas, M.I., Okuda, K.S., Walton, E.M.,
420 Beerman, R.W., Crosier, P.S., and Tobin, D.M. (2015). Interception of host angiogenic
421 signalling limits mycobacterial growth. Nature *517*, 612-615.

422 Passeri, M.J., Cinaroglu, A., Gao, C., and Sadler, K.C. (2009). Hepatic steatosis in response
423 to acute alcohol exposure in zebrafish requires sterol regulatory element binding protein
424 activation. Hepatology *49*, 443-452.
425 Robson, S.C., White, N.W., Aronson, I., Woollgar, R., Goodman, H., and Jacobs, P. (1996).
426 Acute-phase response and the hypercoagulable state in pulmonary tuberculosis. Br J
427 Haematol *93*, 943-949.
428 Russell, D.G., Cardona, P.J., Kim, M.J., Allain, S., and Altare, F. (2009). Foamy
429 macrophages and the progression of the human tuberculosis granuloma. Nat Immunol *10*,
430 943-948.
431 Venkatasubramanian, S., Tripathi, D., Tucker, T., Paidipally, P., Cheekatla, S., Welch, E.,
432 Raghunath, A., Jeffers, A., Tvinnereim, A.R., Schechter, M.E., *et al.* (2016). Tissue factor
433 expression by myeloid cells contributes to protective immune response against
434 Mycobacterium tuberculosis infection. Eur J Immunol *46*, 464-479.
435 Vo, A.H., Swaroop, A., Liu, Y., Norris, Z.G., and Shavit, J.A. (2013). Loss of fibrinogen in
436 zebrafish results in symptoms consistent with human hypofibrinogenemia. PLoS ONE *8*,
437 e74682.
438 Walton, E.M., Cronan, M.R., Beerman, R.W., and Tobin, D.M. (2015). The Macrophage-
439 Specific Promoter mfap4 Allows Live, Long-Term Analysis of Macrophage Behavior during
440 Mycobacterial Infection in Zebrafish. PLoS ONE *10*, e0138949.
441 World Health Organization., and Global Tuberculosis Programme. Global tuberculosis
442 control : WHO report. (Geneva, Global Tuberculosis Programme), p. 15 volumes.
443

444 **Figure legends**

445 **Figure 1: *Mycobacterium marinum* induces coagulation and thrombosis around sites of**
446 **infection in zebrafish**

447 A) Representative images of a *Tg(fabp10a:fgb-EGFP)* embryo infected with *M.marinum*-
448 tdTomato by caudal vein injection, showing clot formation (green) at sites of infection (red)
449 at 3, 4, and 5 DPI. B) Representative images of 5 DPI *Tg(fabp10a:fgb-EGFP)* embryos
450 infected with *M.marinum*-tdTomato WT and ΔESX1 *M. marinum*-td-tomato (ΔESX1)
451 showing clot formation (green) at sites of infection (red). Arrows indicate clotting. C)
452 Quantification of clot formation in burden-matched ΔESX1 mutant-infected *Tg(fabp10a:fgb-*
453 *EGFP)* embryos normalised to WT *M. marinum* control. Error lines represent mean ± SEM,
454 statistical analysis by T test. Data show combined results from two independent experiments.
455 D) Representative images of *Tg(fabp10a:fgb-EGFP)* embryos, where clot formation can be
456 visualised by GFP fluorescence, infected with *M.marinum*-tdTomato (red) and treated with
457 either DMSO or warfarin. E) Quantification of clotting in warfarin-treated *Tg(fabp10a:fgb-*
458 *EGFP)* embryos. F) Quantification of bacterial burden in embryos treated with warfarin. Data
459 are combined results of two independent experiments. F) Representative 2 DPI, 3 DPI and 4
460 DPI images of *Tg(cd41:GFP)* fish infected with *M.marinum*-tdTomato at 3 DPF. White
461 arrow heads show thrombocyte (green) association with areas of bacterial growth (red).
462 Thrombocytes not indicated with an arrow head were circulating and not considered to be
463 associated with bacteria (more detail available in Figure S2C).
464
465 **Figure 2: Anti-platelet drugs reduce bacterial burden in *M. marinum* infection**
466 A) Quantification of bacterial burden in embryos treated with aspirin normalised to DMSO
467 control. Data are combined results of two independent experiments. B) Quantification of
468 bacterial burden in embryos treated with tirofiban normalised to DMSO control. Data are
469 combined results of two independent experiments. C) Quantification of bacterial burden in
470 embryos treated with eptifibatide or DMSO control. D) Representative images of
471 *Tg(cd41:gfp)* embryos treated with tirofiban or DMSO control. E) Quantification of total

thrombocyte *Tg*(*cd41:GFP)* area within the tail of infected larvae treated with tirofiban. F) Quantification of bacterial growth by relative fluorescence in 7H9 broth culture supplemented with drugs as indicated. G) Survival analysis of *P. aerogenosa* PA01 infected embryos treated with anti-platelet drugs as indicated.

All graphs show Mean ± SEM. Statistical analyses performed by T tests and Log-Rank tests where appropriate.

Figure 3: The anti-bacterial effect of anti-platelet drugs is thrombocyte dependent

A) Total fluorescence area of *M. marinum* bacteria in larvae injected with either control or cmpl morpholino (MO) to deplete thrombocytes, and then treated with tirofiban (Tiro). Values are normalised to DMSO-treated control MO larvae. Graphs show the combined results of 2 independent experiments. B) Quantification of bacterial burden in in *itga2b* mutant embryos normalised to WT control. Data are combined results of four independent experiments. C) Quantification of bacterial burden in embryos treated with tirofiban, warfarin, or tirofiban and warfarin, normalised to DMSO control. Data are combined results of two independent experiments. D) Quantification of bacterial burden in $fga^{-/-}$ embryos treated with tirofiban. E) Representative images of 5 DPI *Tg(fabp10a:fgb-EGFP)* embryos infected with *M.marinum*-tdTomato and treated with either DMSO or tirofiban. F) Quantification of clotting relative to bacterial burden in embryos treated with tirofiban normalised to DMSO control. Data are combined results of two independent experiments.

All graphs show Mean ± SEM. Statistical analyses performed by T tests or ANOVA where appropriate.

Figure 4: Thrombocyte activation compromises immunity through granuloma-associated macrophages.

497 A) Quantification of bacterial burden in embryos infected with ΔESX1 *M.marinum*-tdTomato
498 and treated with tirofiban. B) Quantification of bacterial burden at 3 DPI after continuous
499 tirofiban treatment from 0 DPI. C) Quantification of bacterial burden at 5 DPI after overnight
500 drug treatment initiated at 4 DPI. D) Quantification of bacterial burden in embryos infected
501 with *M.marinum*-tdTomato, injected with clodronate liposomes and treated with tirofiban
502 from at 3 DPI. E) Representative images of bacterial granulomas chosen for analysis
503 (bacteria are white in greyscale images), and corresponding Oil Red O (ORO) staining (red-
504 brown in color images). F) Quantification of ORO pixel density relative to granuloma
505 bacterial area, in embryos treated with tirofiban, normalised to DMSO control. G)
506 Representative images of bacterial granulomas showing bacteria in red and TUNEL staining
507 in green. F) Quantification of TUNEL positive area within the largest granuloma of
508 individual embryos.
509 All graphs show Mean ± SEM, statistical tests by T-tests. Data are combined results of two
510 independent experiments, except D) and H) which represent single experiments.
511
512
513 **Graphical abstract.**
514 *M. marinum* indicues two independent haemostatic processes in the zebrafish: ESX1
515 dependent coagulation (1), and ESX1 independent thrombocyte recruitment (2). Bacteria then
516 induce ESX1 dependent thrombocyte activation - either directly or via the macrophage - (3),
517 and this leads to foam cell formation and macrophage necrosis, promoting bacterial growth
518 (4). Inhibition of thrombocyte activation with anti-platelet drugs like Tirofiban, stops this
519 progression and thereby limits the growth of bacteria. Drugs which reduce coagulation (1)
520 have no effect on bacterial growth.
521

522

523 **Supplementary Figure Legends**

524 **Figure S1**

525 Related to Figure 1. Quantification of clot formation in warfarin-treated embryos infected
526 with *M. marinum.* Error lines represent mean ± SEM, statistical analysis by T test.

527

528 **Figure S2**

529 Related to Figure 1. A) Representative images of 5 DPI *Tg(cd41:GFP)* embryos infected
530 with *M.marinum*-tdTomato, showing thrombocyte accumulation (green) at sites of bacterial
531 infection (red). B) Quantification of total thrombocyte *Tg*(*cd41:GFP)* area within the tail of
532 uninfected or WT *M.marinum*-tdTomato infected embryos. C) Correlation between *M.*
533 *marinum* bacterial burden and total thrombocyte *Tg*(*cd41:GFP)* area within the tail of
534 infected embryos. D) Quantification of total thrombocyte *Tg*(*cd41:GFP)* area within the tail
535 of uninfected or ΔESX1 *M.marinum*-tdTomato infected larvae at 5 DPI. E) Correlation
536 between ΔESX1 *M. marinum* bacterial burden and total thrombocyte *Tg* (*cd41:GFP)* area
537 within the tail of infected embryos at 5 DPI.

538

539 **Figure S3**

540 Related to Figure 1. Images of 2 DPI, 3 DPI and 4 DPI *Tg(cd41:GFP)* embryos infected with
541 *M.marinum*-tdTomato at 3 DPF. At each time-point, 2 images were taken ~10 seconds apart.
542 Thrombocytes located in the same position in both images were considered stationary (non-
543 circulating), and labelled with a white arrow head.
544 Graphs show Mean ± SEM, statistical testing by T-test or linear regression.

545

546 **Figure S4**

Related to Figure 2. A) Representative images of thrombocyte accumulation at tail wound in 4 DPF *Tg(cd41:GFP)* embryos , 4 hours post injury (hpi). B) Quantification of thrombocytes within 100 μm of the cut site 4 hpi in aspirin-treated embryos. C) Quantification of thrombocytes within 100 μm of the cut site 4 hpi in tirofiban-treated embryos.

Graphs show Mean ± SEM, statistical testing by T-test (B and C) or ANOVA (D).

Figure S5

Related to Figure 3. A) Quantification of thrombocytes within 100 μm of the cut site 4 hours after injury in *itga2b* WT, heterozygous and knock-out embryos. B) Representative images of *Tg(cd41:gfp) itga2b* mutant embryos infected with *M. marinum*-tdTomato. C) Quantification of total thrombocyte *Tg*(*cd41:GFP)* area within the tail of infected *itga2b* mutant embryos.

Figure S6

Related to Figure 4. A) Quantification of bacterial burden in embryos infected with a low dose of 10-50 fluorescent *M. marinum* and treated with tirofiban. **B)** Representative images of caudal haematopoietic tissue in 6 DPF *Tg(mfap4:tdTomato)* embryos, where macrophages are fluorescently labelled, injected with clodronate or PBS liposomes at 4 DPF. **C)** Quantification of macrophage number by fluorescent pixel count at 5 DPI in embryos injected with clodronate or PBS liposomes at 3 DPI, and treated with tirofiban. Graphs show Mean ± SEM, statistical tests by T-tests (A and B) or ANOVA (D).

Methods

Zebrafish husbandry

Adult zebrafish were housed at the Garvan Institute of Medical Research Biological Testing Facility (St Vincent's Hospital AWC Approval 1511) and embryos were produced by natural

572 spawning for infection experiments at the Centenary Institute (Sydney Local Health District
573 AWC Approval 2016-022). Zebrafish embryos were obtained by natural spawning and
574 embryos were raised at 28°C in E3 media.
575
576 *Zebrafish lines*
577 Wild type zebrafish are the TAB background. Transgenic lines are: *Tg(fabp10a:fgb-*
578 *EGFP)*^{mi4001} referred to as *Tg(fabp10a:fgb-EGFP)(Vo et al., 2013)*, *Tg(-6.0itga2b:eGFP)*^{la2}
579 referred to as *Tg(cd41:EGFP)(Lin et al., 2005)*, *Tg(mfap4:tdTomato)*^{xt12} referred to as
580 *Tg(mfap4:tdTomato)(Walton et al., 2015)*, Mutant allele *fga*^{mi} contains a 26 bp insertion in
581 the *fibrinogen alpha chain* gene (manuscript in preparation).
582
583 *Infection of zebrafish embryos*
584 Aliquots of single cell suspensions of midlog-phase *Mycobacterium marinum* M strain,
585 ΔESX1 *M. marinum* and *Pseudomonas aeruginosa* PA01 were frozen at -80°C for use in
586 infection experiments. Bacterial aliquots were thawed and diluted with phenol red dye (0.5%
587 w/v). 10-15 nL was injected into the caudal vein or trunk of M-222 (tricaine)-anaesthetised
588 30-48 hpf embryos resulting in a standard infectious dose ~400 fluorescent *M. marinum*.
589 Embryos were recovered into E3 supplemented with 0.036 g/L PTU, housed at 28 °C and
590 imaged on day 5 of infection unless otherwise stated.
591
592 *Drug treatments*
593 Embryos were treated with vehicle control (DMSO or water as appropriate), 10 µg/ml
594 aspirin, 20 µg/ml tirofiban, 10 µM eptifibatide, or 5 µM warfarin. Drugs and E3 were
595 replaced on days 0, 2, and 4 days post infection (DPI) unless otherwise stated.
596

Tail wound thrombosis assay

Three day post fertilisation (DPF) embryos were treated over-night with anti-platelet drugs. They were anaesthetised, and then a small amount of their tail was removed with a scalpel. Embryos were imaged 4 hours post wounding and the number of GFP positive cells within 100 μm of the cut site was counted.

Imaging

Live zebrafish embryos were anaesthetized in M-222 (Tricaine) and mounted in 3% methylcellulose for imaging on a Leica M205FA or DM6000B fluorescence stereomicroscope. Image analysis was carried out with Image J Software Version 1.51j using fluorescent pixel counts and intensity measurements as previously described (Matty et al., 2016).

Axenic culture

A midlog culture of fluorescent *M. marinum* was diluted 1:100 and aliquoted into 96 well plates for drug treatment. Cultures were maintained at 28°C in a static incubator and bacterial fluorescence was measured in a plate reader.

Morpholinos:

Embryos were injected at the single cell stage with 1 pmol cMPL (5′-CAGAACTCTCACCCTTCAATTATAT-3′), or control morpholino (5′-CCTCTTACCTCAGTTACAATTTATA-3′).

Clodronate liposome injections:

Larvae were injected at 3 DPI (4 DPF) with 10 nl of 5 mg/ml clodronate liposomes or 5 mg/ml PBS vehicle liposomes by caudal vein injection.

Oil-red O:

Oil Red O lipid staining on whole mount embryos was performed and analysed as previously described (Johansen et al., 2018; Passeri et al., 2009). Briefly, embryos were individually imaged for bacterial distribution by fluorescent microscopy, fixed, and stained in Oil Red O (0.5% w/v in propylene glycol). Oil Red O density was calculated by using the 'measure' function in Image J, and subtracting the mean brightness of a representative region within each granuloma from the mean brightness of a representative adjacent 'background' region.

Statistics

All t-tests were unpaired t-tests with Welch's correction. All ANOVA were ordinary one-way ANOVA, comparing the mean of each group with the mean of every other group, using Turkey's multiple comparisons test with a single pooled variance. In cases where data was pooled from multiple experiments, data from each was normalised to its own within-experiment control (usually 'DMSO') before pooling. Outliers were removed using ROUT, with Q=1%.

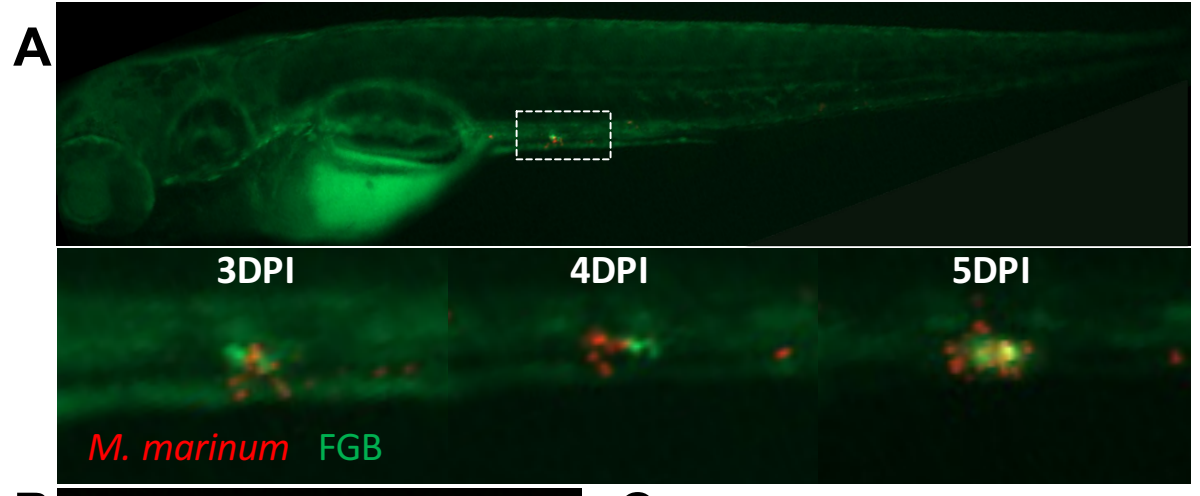
A
3DPI
4DPI
5DPI
M. marinum FGB

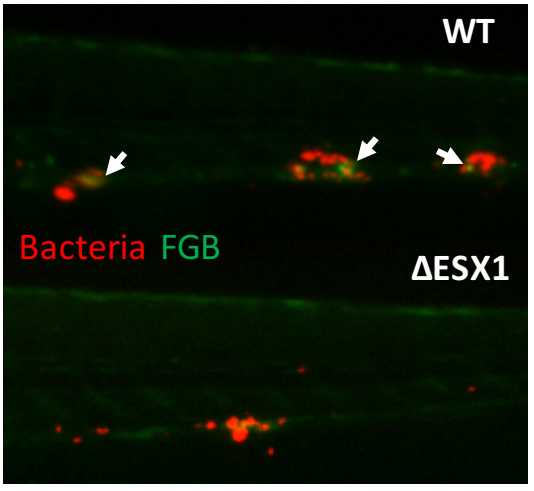
B
WT
Bacteria FGB
ΔESX1

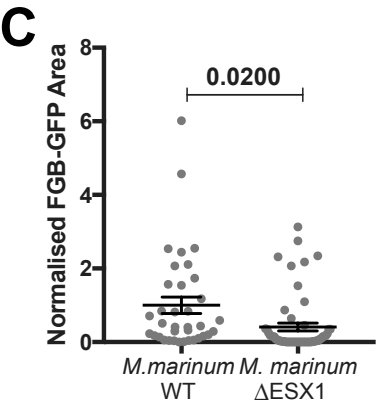
C
Normalised FGB-GFP Area
0.0200
M.marinum WT
M. marinum ΔESX1

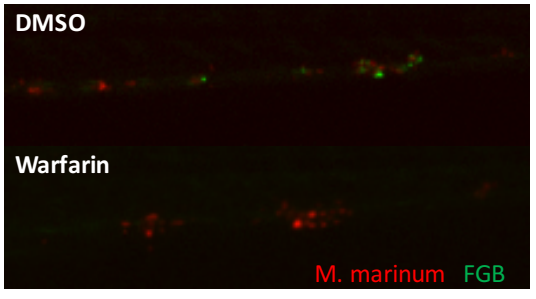
D
DMSO
Warfarin
M. marinum FGB

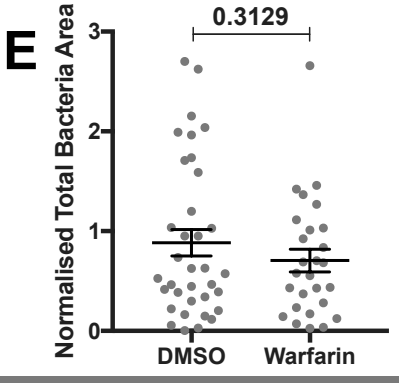
E
Normalised Total Bacteria Area
0.3129
DMSO
Warfarin

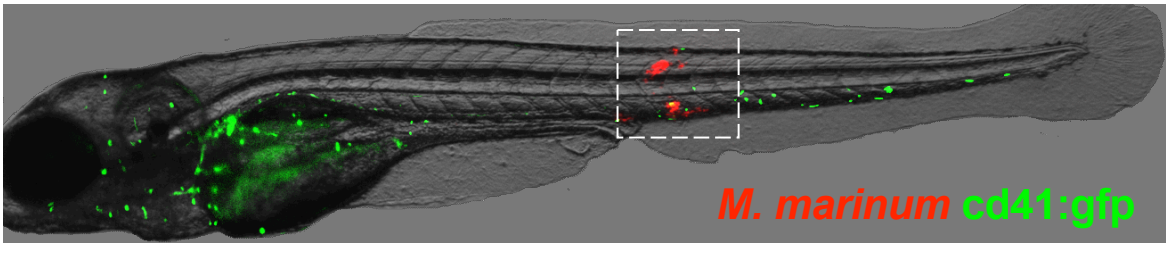
F
M. marinum cd41:gfp

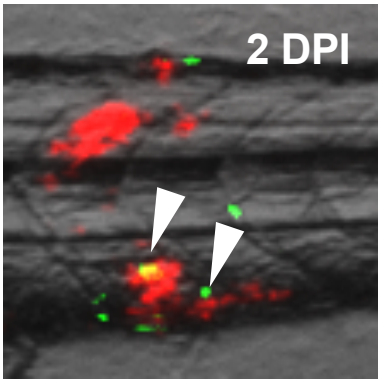
2 DPI

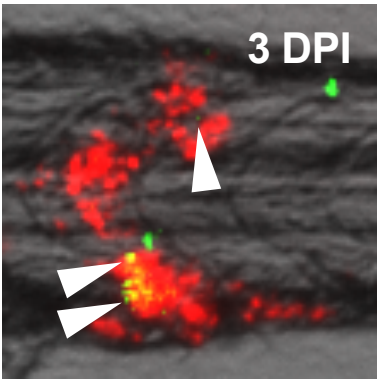
3 DPI

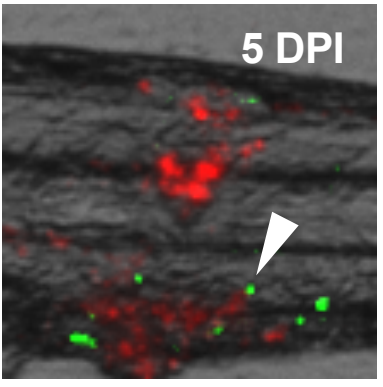
5 DPI

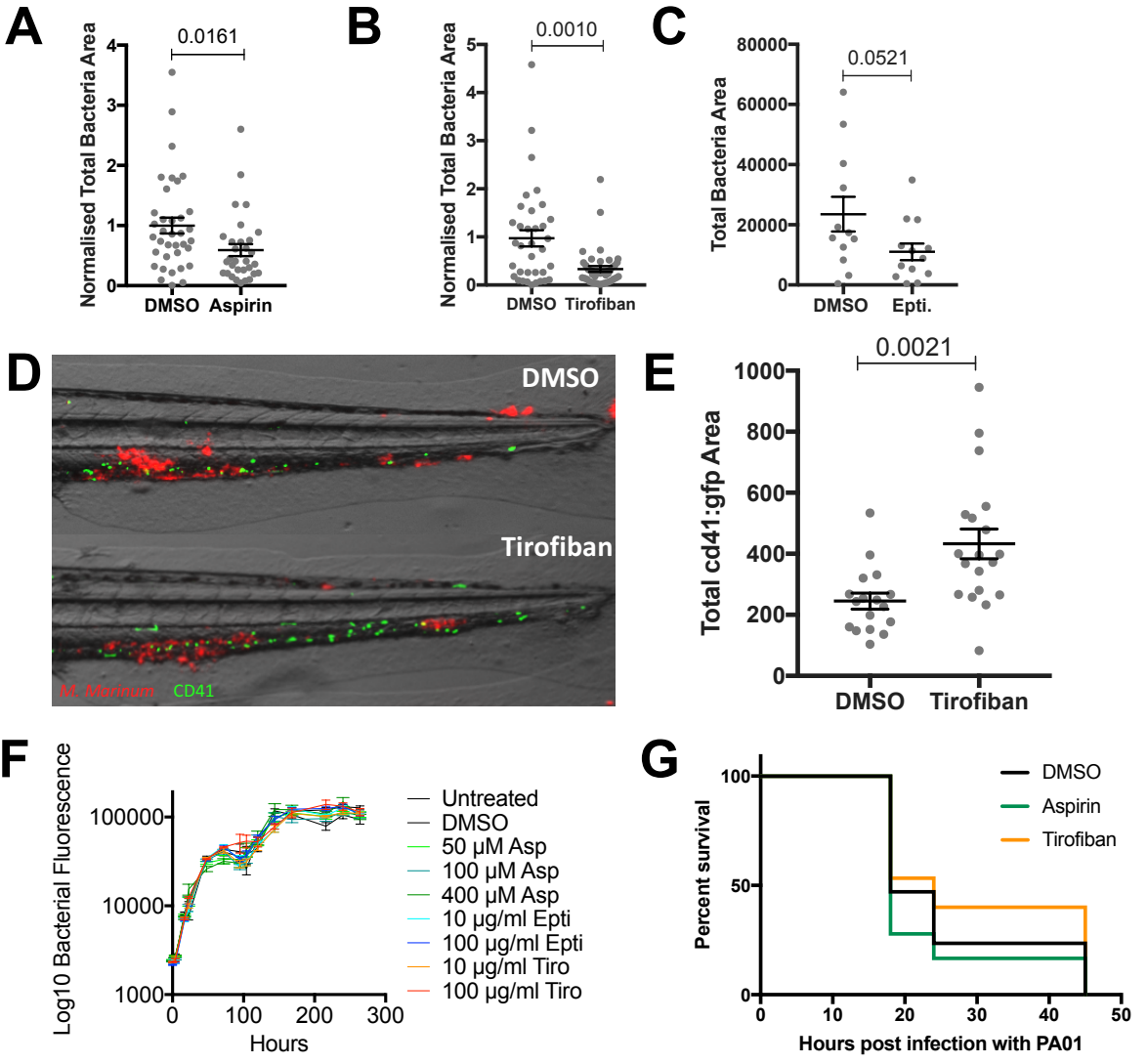
A
Normalised Total Bacteria Area
0.0161
DMSO
Aspirin
B
Normalised Total Bacteria Area
0.0010
DMSO
Tirofiban
C
Total Bacteria Area
0.0521
DMSO
Epti.
D
DMSO
Tirofiban
M. Marinum
CD41
E
Total cd41:gfp Area
0.0021
DMSO
Tirofiban
F
Log10 Bacterial Fluorescence
Hours
Untreated
DMSO
50 µM Asp
100 µM Asp
400 µM Asp
10 µg/ml Epti
100 µg/ml Epti
10 µg/ml Tiro
100 µg/ml Tiro
G
Percent survival
Hours post infection with PA01
DMSO
Aspirin
Tirofiban

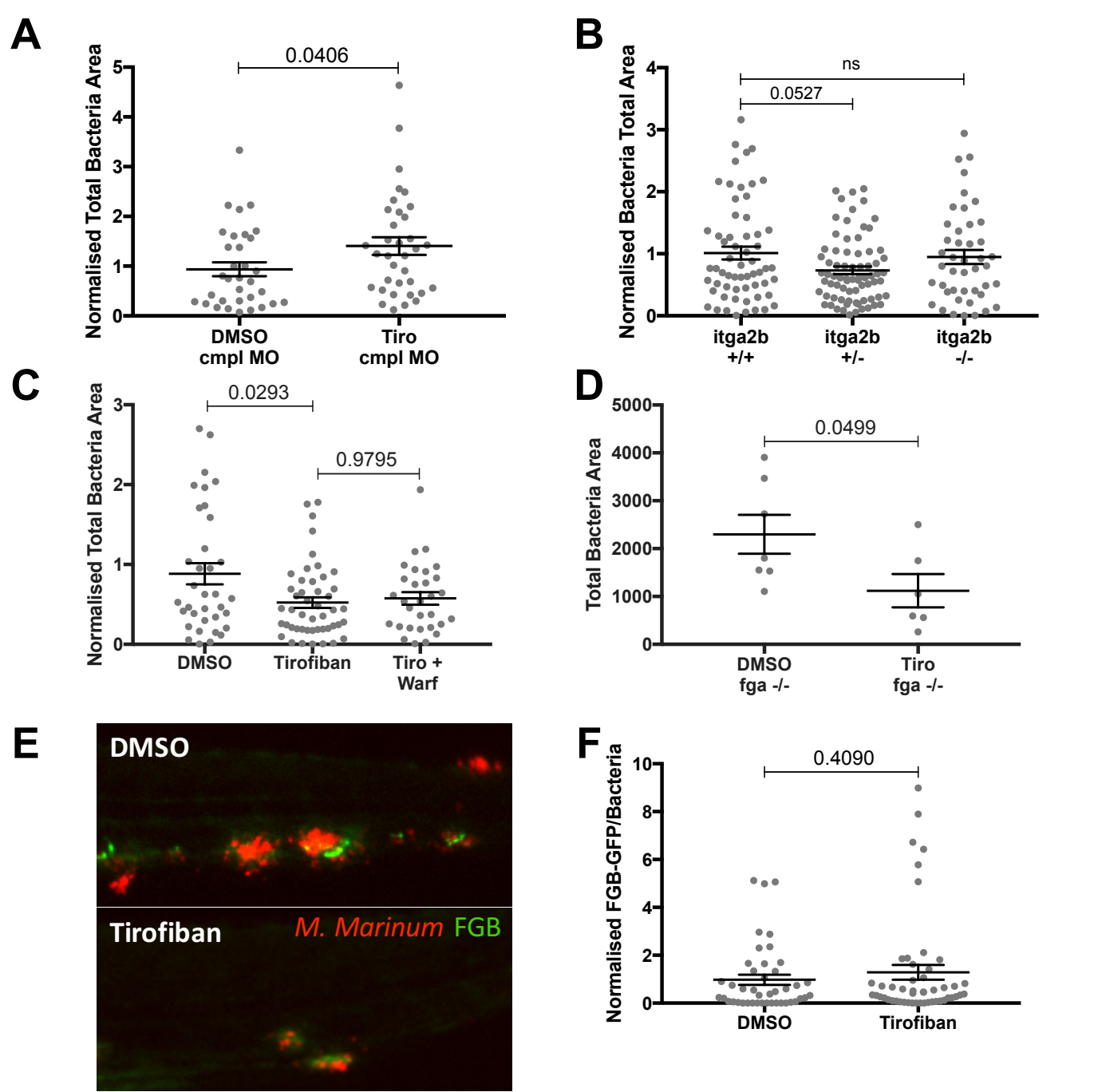
A
Normalised Total Bacteria Area
0.0406
DMSO cmpl MO
Tiro cmpl MO
B
Normalised Bacteria Total Area
ns
0.0527
itga2b +/+
itga2b +/-
itga2b -/-
C
Normalised Total Bacteria Area
0.0293
0.9795
DMSO
Tirofiban
Tiro + Warf
D
Total Bacteria Area
0.0499
DMSO fga -/-
Tiro fga -/-
E
DMSO
Tirofiban
M. Marinum FGB
F
Normalised FGB-GFP/Bacteria
0.4090
DMSO
Tirofiban

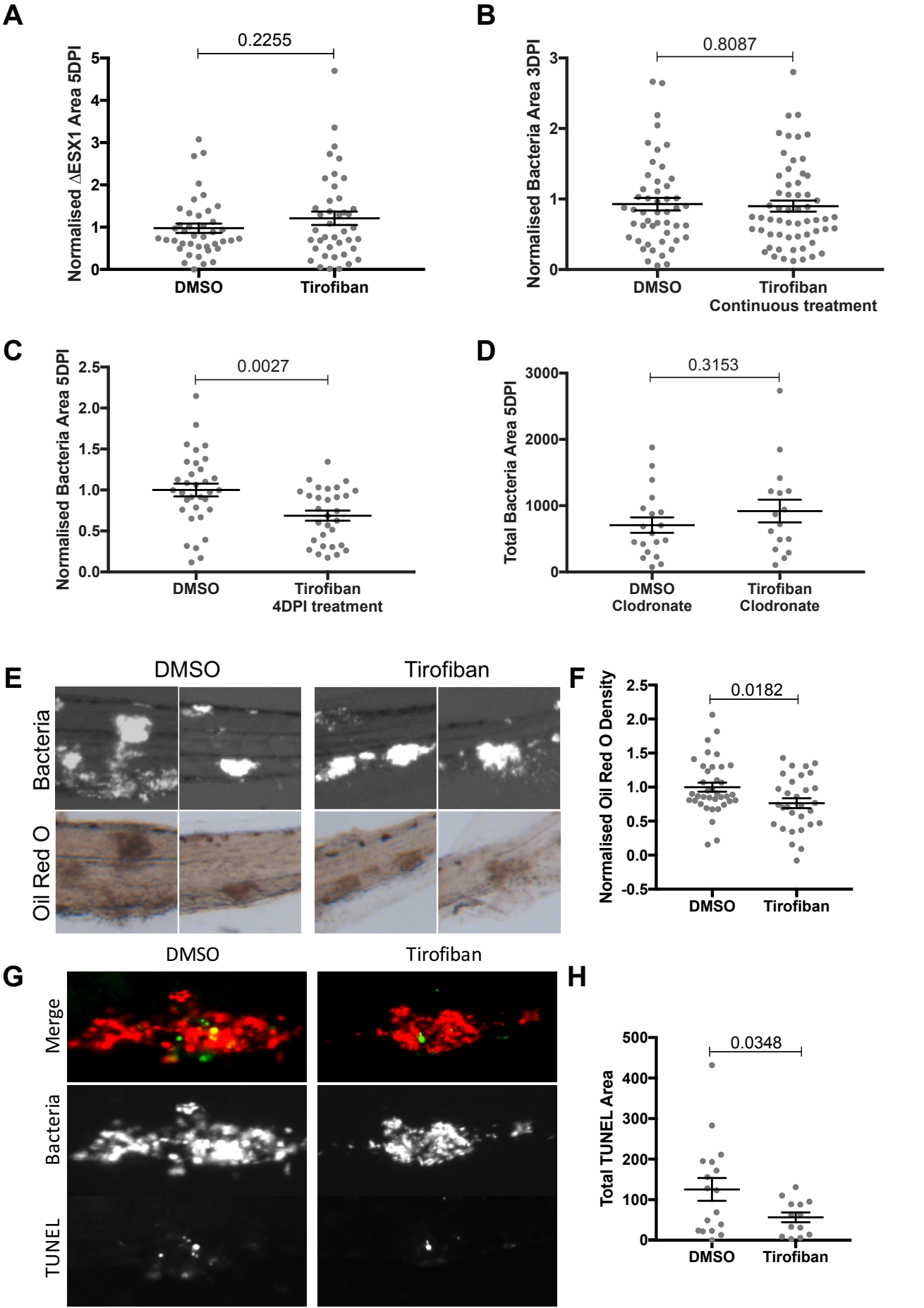
A
0.2255
Normalised ΔESX1 Area 5DPI
DMSO
Tirofiban
B
0.8087
Normalised Bacteria Area 3DPI
DMSO
Tirofiban
Continuous treatment
C
0.0027
Normalised Bacteria Area 5DPI
DMSO
Tirofiban
4DPI treatment
D
0.3153
Total Bacteria Area 5DPI
DMSO
Clodronate
Tirofiban
Clodronate
E
DMSO
Tirofiban
Bacteria
Oil Red O
F
0.0182
Normalised Oil Red O Density
DMSO
Tirofiban
G
DMSO
Tirofiban
Merge
Bacteria
TUNEL
H
0.0348
Total TUNEL Area
DMSO
Tirofiban

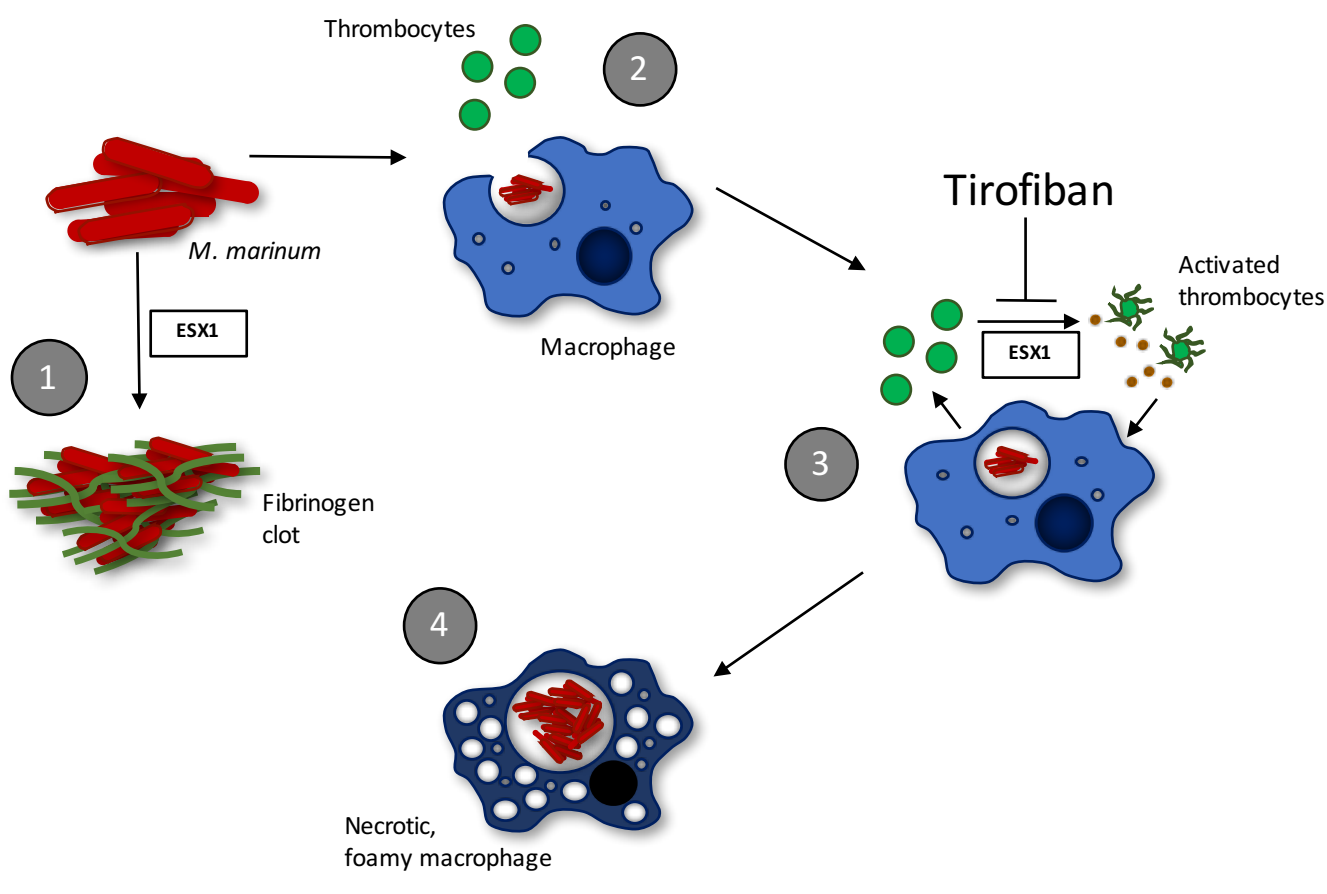
Thrombocytes
2
M. marinum
ESX1
1
Macrophage
Tirofiban
Activated
thrombocytes
ESX1
3
Fibrinogen
clot
4
Necrotic,
foamy macrophage

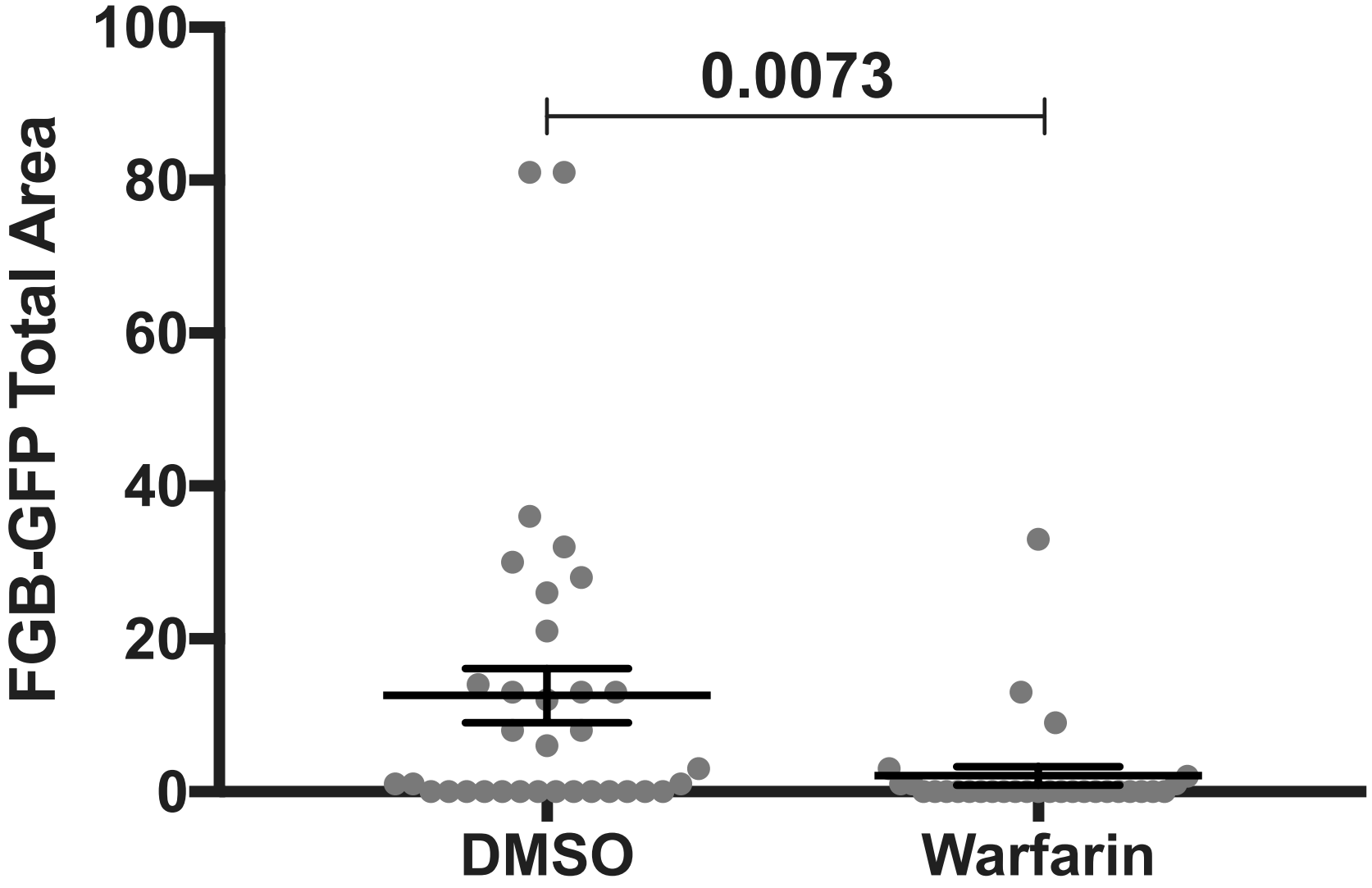
FGB-GFP Total Area
100
80
60
40
20
0
0.0073
DMSO
Warfarin

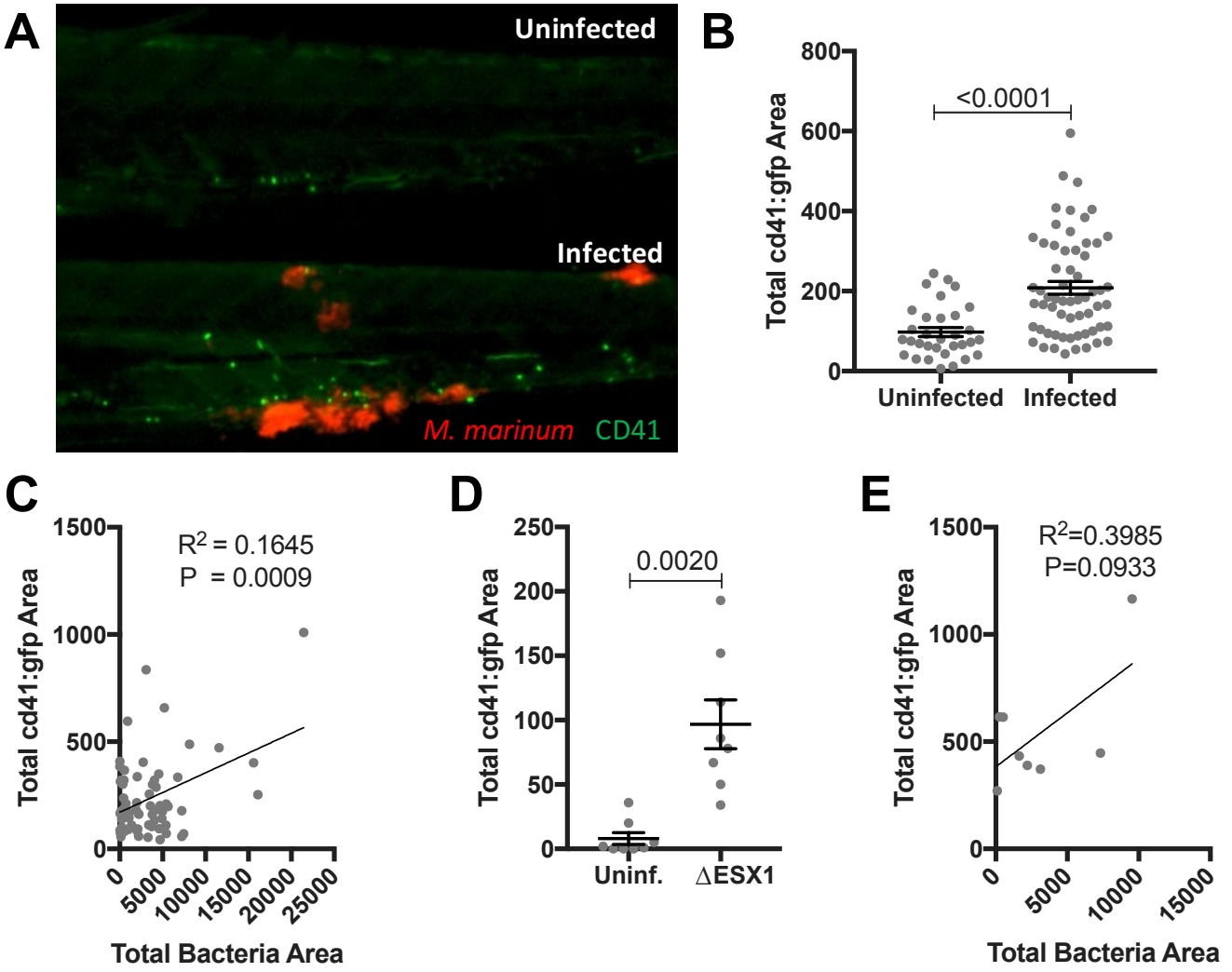
A
Uninfected
Infected
M. marinum
CD41
B
Total cd41:gfp Area
800
600
400
200
0
<0.0001
Uninfected
Infected
C
Total cd41:gfp Area
1500
1000
500
0
R2 = 0.1645
P = 0.0009
0
5000
10000
15000
20000
25000
Total Bacteria Area
D
Total cd41:gfp Area
250
200
150
100
50
0
0.0020
Uninf.
ΔESX1
E
Total cd41:gfp Area
1500
1000
500
0
R2=0.3985
P=0.0933
0
5000
10000
15000
Total Bacteria Area

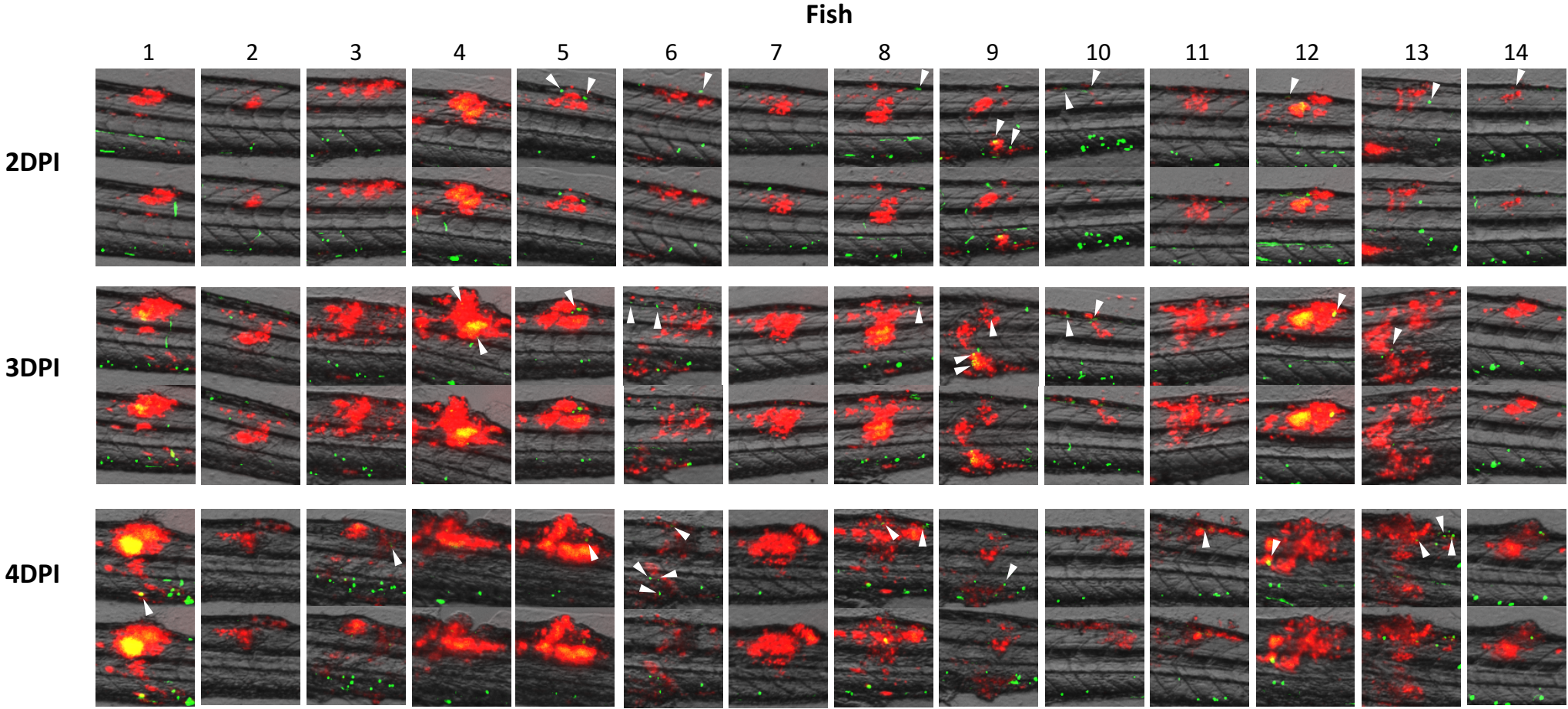
Fish
1
2
3
4
5
6
7
8
9
10
11
12
13
14
2DPI
3DPI
4DPI

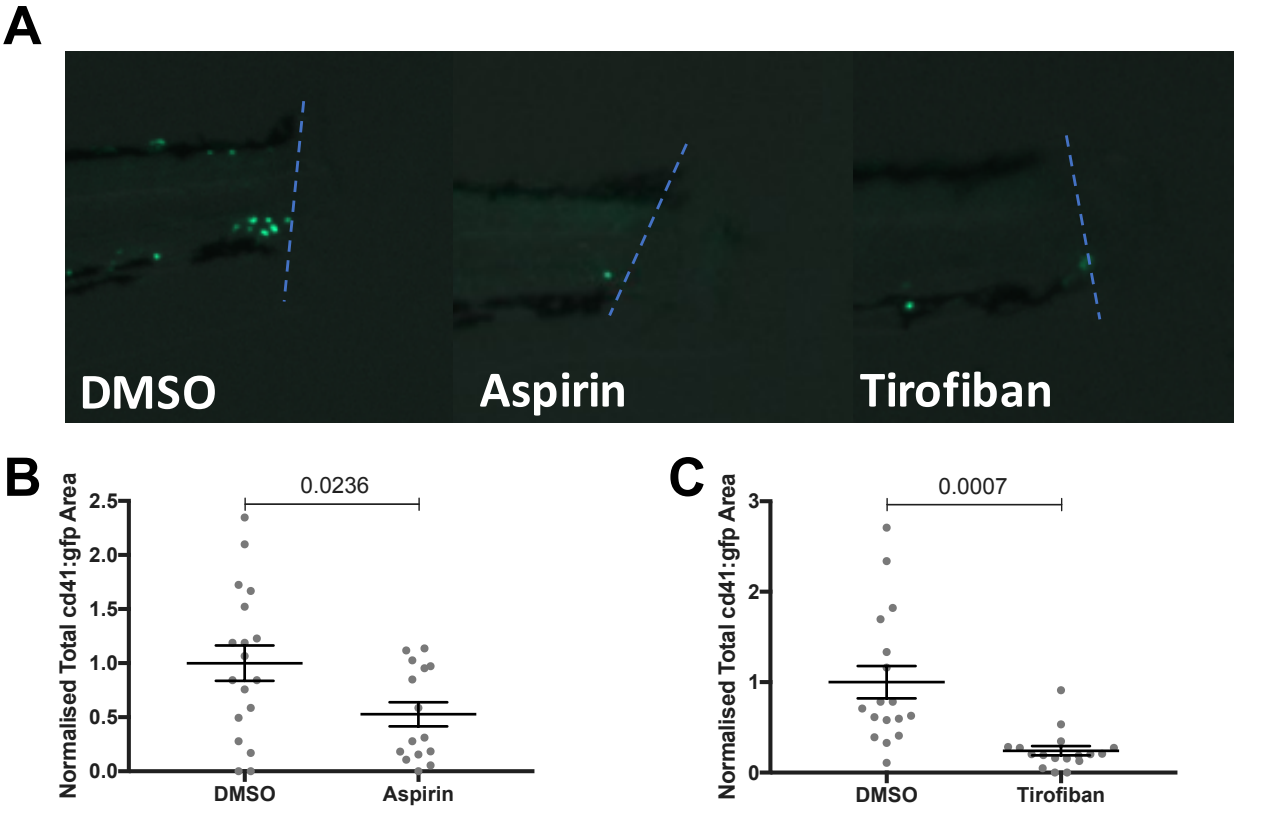
A
DMSO
Aspirin
Tirofiban
B
Normalised Total cd41:gfp Area
0.0236
2.5
2.0
1.5
1.0
0.5
0.0
DMSO
Aspirin
C
Normalised Total cd41:gfp Area
0.0007
3
2
1
0
DMSO
Tirofiban

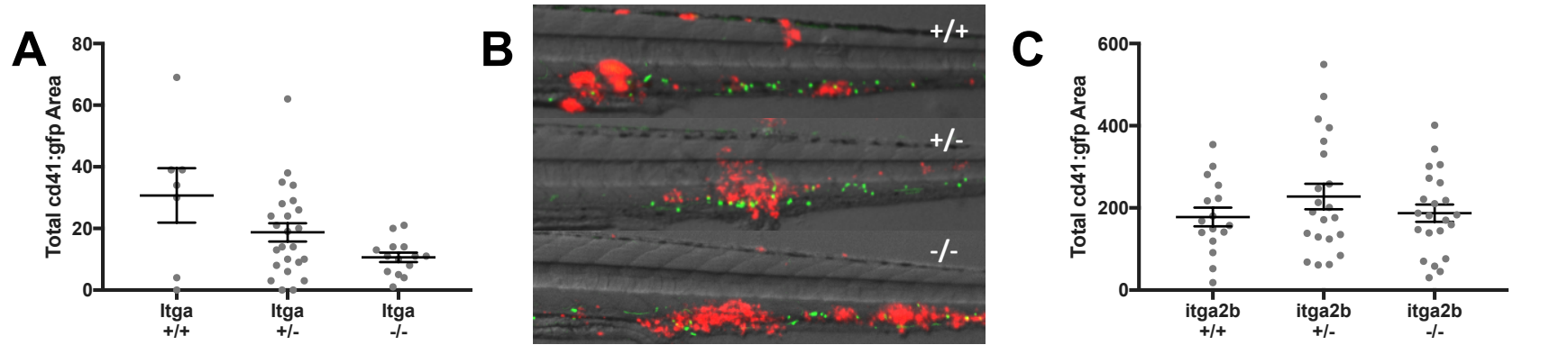
A
Total cd41:gfp Area
80
60
40
20
0
Itga
+/+
Itga
+/-
Itga
-/-
B
+/+
+/-
-/-
C
Total cd41:gfp Area
600
400
200
0
itga2b
+/+
itga2b
+/-
itga2b
-/-

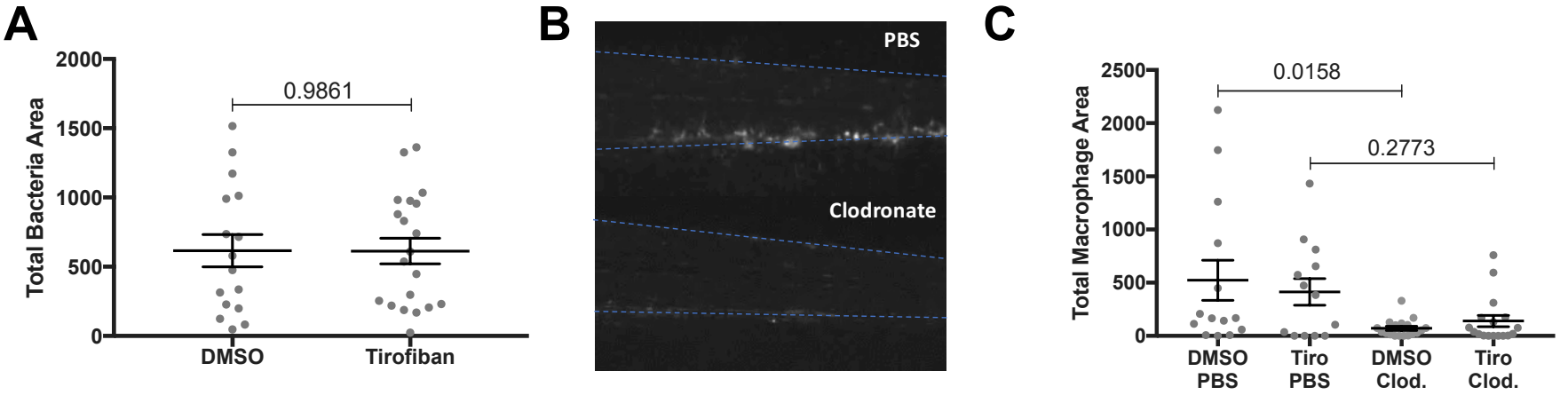
A
Total Bacteria Area
2000
1500
1000
500
0
0.9861
DMSO
Tirofiban
B
PBS
Clodronate
C
Total Macrophage Area
2500
2000
1500
1000
500
0
0.0158
0.2773
DMSO PBS
Tiro PBS
DMSO Clod.
Tiro Clod.